PHYSICAL REVIEW E, VOLUME 65, 016204

Fractal properties of the lattice Lotka-Volterra model

G. A. Tsekouras[1,2] and A. Provata[1,*]
[1]Institute of Physical Chemistry, National Research Center "Demokritos," 15310 Athens, Greece
[2]Department of Physics, University of Athens, 10679 Athens, Greece

(Received 19 April 2001; revised manuscript received 12 July 2001; published 14 December 2001)

The lattice Lotka-Volterra (LLV) model is studied using mean-field analysis and Monte Carlo simulations. While the mean-field phase portrait consists of a center surrounded by an infinity of closed trajectories, when the process is restricted to a two-dimensional (2D) square lattice, local inhomogeneities/fluctuations appear. Spontaneous local clustering is observed on lattice and homogeneous initial distributions turn into clustered structures. Reactions take place only at the interfaces between different species and the borders adopt locally fractal structure. Intercluster surface reactions are responsible for the formation of local fluctuations of the species concentrations. The box-counting fractal dimension of the LLV dynamics on a 2D support is found to depend on the reaction constants while the upper bound of fractality determines the size of the local oscillators. Lacunarity analysis is used to determine the degree of clustering of homologous species. Besides the spontaneous clustering that takes place on a regular 2D lattice, the effects of fractal supports on the dynamics of the LLV are studied. For supports of dimensionality $D_s < 2$ the lattice can, for certain domains of the reaction constants, adopt a poisoned state where only one of the species survives. By appropriately selecting the fractal dimension of the substrate, it is possible to direct the system into a poisoned or oscillatory steady state at will.

DOI: 10.1103/PhysRevE.65.016204 PACS number(s): 05.45.−a, 05.45.Df, 05.65.+b, 05.10.−a

I. INTRODUCTION

It is now well established [1] that mean-field approaches used traditionally for the description of reactive processes are not adequate to describe the rich complex dynamical behavior and the local fluctuations of processes restricted on low-dimensional supports [2–7].

In particular, catalytic chemical reactions are one category of restricted reactive processes where the reactions can only take place if the reactive species are adsorbed on the surface of the catalyst. For these processes basic mean-field requirements such as homogeneity and high diffusivity do not hold since reactions are only possible between neighboring molecules. Well known catalytic reactions of this type are the CO oxidization on the surface of Pt [8–10], the NO reduction on the surface of Pt [10–13], and the NO+CO reaction on Pt [14,15]. To overcome the difficulties arising at the mean-field level, specific simulation models have been constructed that take explicitly into account both the structural properties of the support and the local nature of the interactions. One well known model is the ZGB model for the CO oxidation on Pt surface [16]. This model predicts periodic and transient behaviors that correspond to poisoning phenomena [6,17–22]. Along the same lines are simulations with surface restructuring [6,7,23] and superlattice ordering [24]. Also, the $NO+H_2$ reaction has been studied using lattice gas models [25] on substrates with different properties [26]. All these studies predict the appearance of complex local patterns, poisoning transitions, and periodic or chaotic oscillations.

In a recent work, the effort to study the origin of the complexity of catalytic processes was undertaken using a simple bimolecular open reactive system, the lattice Lotka-Volterra model(LLV) [2]. The original Lotka-Volterra model was first introduced in order to describe the dynamics of a system of competitive biological species (see Ref. [27]). It was very successful in the sense that due to its nonlinear structure it was able to describe oscillatory schemes. At the time the model was proposed, nonlinear oscillations had already been recorded at ecological systems *in vivo*. The Lotka-Volterra is a mean-field model that contains one bimolecular autocatalytic reactive step, one creation step, and one annihilation step. At the mean-field level it predicts a phase portrait consisting of a center surrounded by a continuum of closed curves.

Simple, space-dependent, autocatalytic reaction models, such as the general epidemic process, have been studied by Grassberger [28] using Monte Carlo methods. These models predict criticality and propagating waves on 2D supports. Excitable media, most often modeled by reaction-diffusion processes, are alternative examples exhibiting propagating patterns on low-dimensional supports. Furthermore, excitable media present a high degree of spatial organization [7,29] and have been studied as percolation problems [30,31] exhibiting spontaneous fractality.

The original Lotka-Volterra model, being a mean-field model is space independent and cannot be directly realized on lattice because the condition of conservation of space (total number of lattice sites where the reactions take place) does not hold. For this reason one of the current authors (A.P.) and collaborators have introduced the LLV model [2]. In the LLV model there are two kinds of reacting molecules as well as the empty lattice sites. All three reactions consist of bimolecular steps and three species X_1, X_2, and S are participating. X_1 and X_2 are considered as on-lattice adsorbed species, while S denotes the empty lattice sites. The LLV scheme is the following [2]:

---

*Corresponding author.
Email address: aprovata@mail.demokritos.gr

1063-651X/2001/65(1)/016204(8)/$20.00

$$X_1+X_2\xrightarrow{k_s}2X_2, \tag{1a}$$

$$X_2+S\xrightarrow{k_1}2S, \tag{1b}$$

$$S+X_1\xrightarrow{k_2}2X_1. \tag{1c}$$

Step (1a) represents an autocatalytic reaction between species X_1 and X_2 while the second step (1b) denotes desorption of a particle X_2 and creation of an empty site S provided that there is a second empty site S in the neighborhood. Similarly, the third reaction (1c) stands for a cooperative adsorption. An empty site S is filled by species X_1 provided that a X_1 is already adsorbed on a neighboring site.

If x_1, x_2, and s stand for the total concentration of molecules X_1, X_2, and empty sites, respectively, then the dynamics of the LLV model is represented by

$$\frac{dx_1}{dt}=k_2x_1s-k_sx_1x_2, \tag{2a}$$

$$\frac{dx_2}{dt}=k_sx_2x_1-k_1x_2s, \tag{2b}$$

$$\frac{ds}{dt}=k_1x_2s-k_2x_1s. \tag{2c}$$

This dynamical system has already been investigated thoroughly [2]. Due to its construction one can immediately recognize that there is a constant of motion:

$$C=x_1+x_2+s=1. \tag{3}$$

This constant C corresponds to the total number of lattice sites that either contain particles (X_1 or X_2) or empty sites (S). For $C=1$ the conservation condition, Eq. (3), represents the probability conservation on every lattice site: one lattice site contains either X_1 with probability x_1, X_2 with probability x_2, or S with probability $s=1-x_1-x_2$.

Using Eq. (3) one may eliminate the dynamical function $s(t)$ and obtain the following 2D nonlinear system

$$\frac{dx_1}{dt}=k_2x_1\left(1-x_1-\frac{k_2+k_s}{k_2}x_2\right), \tag{4a}$$

$$\frac{dx_2}{dt}=-k_1x_2\left(1-x_2-\frac{k_1+k_s}{k_1}x_1\right). \tag{4b}$$

This dynamical system has four fixed points, three of which are saddle points and one is a center [2]. The saddle points are (0,0), (0,1), (1,0) while the center is $[k_1/(k_1+k_2+k_s),k_2/(k_1+k_2+k_s)]$. The center is surrounded by a continuum of closed trajectories. The phase portrait of the system is shown in Fig. 1. Further investigations have shown that the dynamical system is conservative for any values of k_1,k_2,k_s while for the special case $k_1=k_2=k_s$ it is Hamiltonian [32,33].

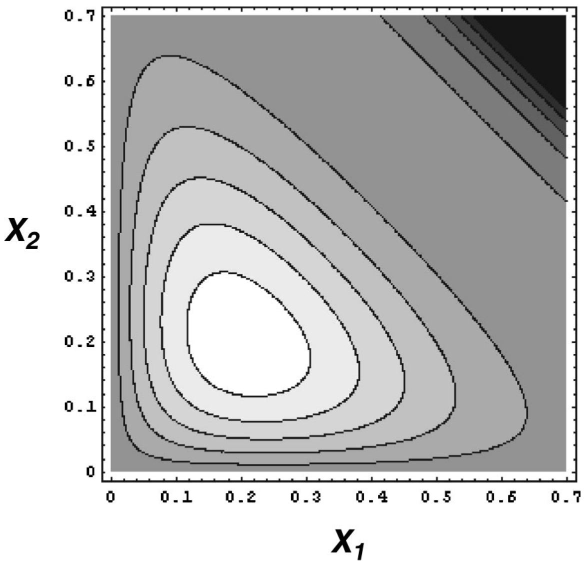

FIG. 1. Phase space of the LLV model for $k_1=0.3$, $k_2=0.3$, $k_s=0.9$ (or $a_1=0.2$, $a_2=0.2$).

By appropriate rescaling of the parameters and the time variable it is possible to obtain a minimal parameter space as follows:

$$a_1=\frac{k_1}{k_1+k_2+k_s}, \tag{5a}$$

$$a_2=\frac{k_2}{k_1+k_2+k_s}, \tag{5b}$$

$$\tau=t(k_1+k_2+k_s). \tag{5c}$$

Using Eqs. (5), Eqs. (2) are reduced to

$$\frac{dx_1}{d\tau}=x_1[a_2s-(1-a_1-a_2)x_2], \tag{6a}$$

$$\frac{dx_2}{d\tau}=x_2[(1-a_1-a_2)x_1-a_1s], \tag{6b}$$

$$\frac{ds}{d\tau}=s(a_1x_2-a_2x_1). \tag{6c}$$

Using Eq. (3), s is eliminated from Eqs. (6) and the LLV system is finally reduced to

$$\frac{dx_1}{d\tau}=a_2x_1\left(1-x_1-\frac{1-a_1}{a_2}x_2\right), \tag{7a}$$

$$\frac{dx_2}{d\tau}=-a_1x_2\left(1-\frac{1-a_2}{a_1}x_1-x_2\right). \tag{7b}$$

Equations (6) and (7) describe the dynamical system with the minimal number of parameters and it is not possible to further reduce the parametric space using any other rescaling. In the new parameter space the center is now positioned

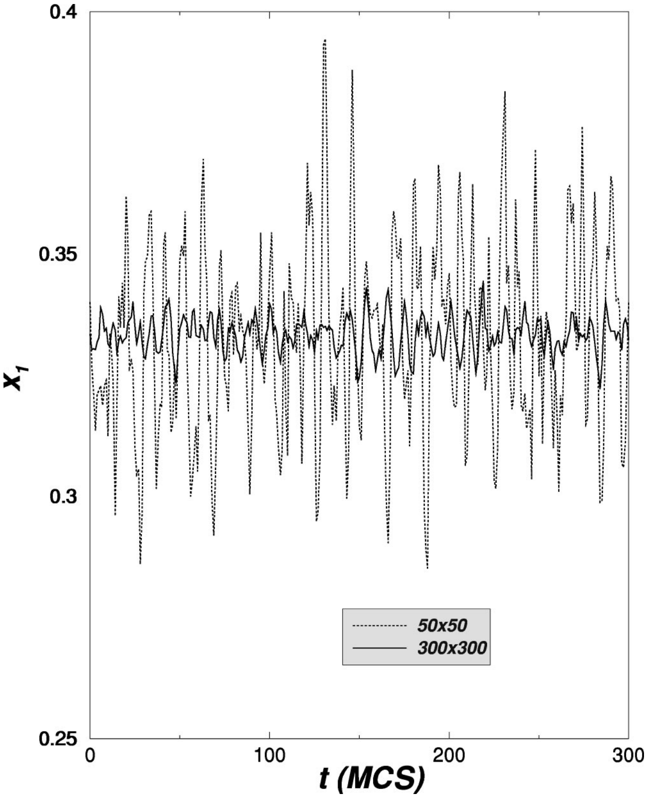

FIG. 2. Oscillations on a 300×300 lattice and on a 50×50 sublattice.

at $(a_1, a_2, 1-a_1-a_2)$. Comparison with simulation data can always be performed by inverting this parameter rescaling.

In order to study the local behavior of the system, Monte Carlo simulations were used on a square lattice of size $L\times L$, with periodic boundary conditions. The algorithm chosen was the one originally used for studying LLV [2]. Specifically, at every timestep a random site is picked and its four nearest neighbors are checked for compatibility with the LLV reactions (1a), (1b), and (1c). Reactions take place with probability $k_i, i=1,2,s$. After completing this procedure a new random site is chosen. One Monte Carlo step (MCS) is completed after a number of trials equal to the total number of lattice sites $(L\times L)$.

Using the above method it has been demonstrated that while kinetic oscillations are almost totally suppressed after a certain time in large lattices, it appears that they are conserved in small scales (Fig. 2). It seems that for small regions there exist "local oscillators" that follow the behavior described by mean-field equations quite closely. These local oscillators, however, tend to be out of phase and the net result is that throughout the lattice no global oscillations can be observed.

In the current work the characteristics of the local oscillators are studied, together with their sensitivity to initial conditions, variation of their size depending on the reactivity constants k_i and possible fractal structure of the substrate. Also certain spatiotemporal phenomena that are manifestly displayed by the system are investigated.

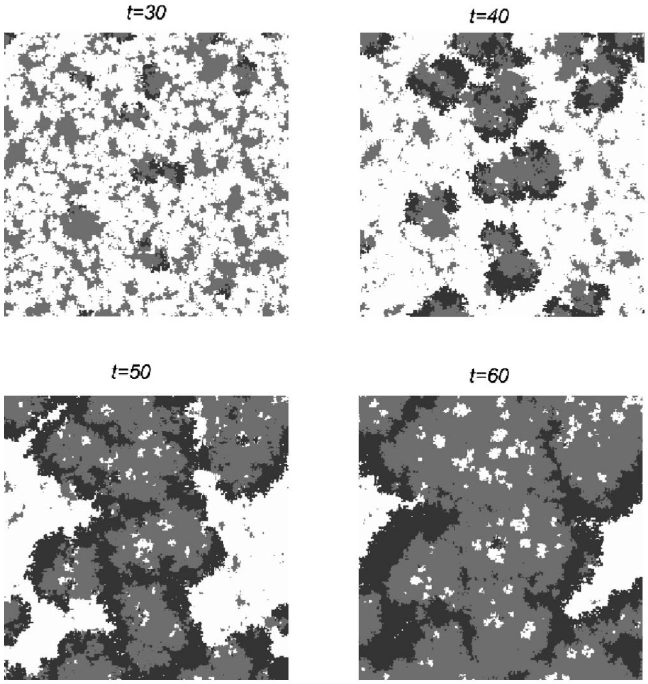

FIG. 3. A visual representation of the lattice for $t=30$, 40, 50, and 60 (MCS). The reaction constants are $k_1=0.9$, $k_2=0.3$, $k_3=0.1$ $(a_1=0.692,\ a_2=0.231)$.

In particular, in Sec. II the fractal structures developed on the square lattice as a result of local fluctuations are studied and the characteristic length of the local oscillators is calculated. An explanation of the global lattice behavior based on this hypothesis is proposed. In Sec. III, in order to simulate the LLV dynamics on microstructured catalytic surfaces both deterministic and random fractal substrates are introduced and the dynamical behavior that arises is examined. Finally, in Sec. IV our main conclusions are recapitulated and certain aspects concerning the reverse model and the effect of mixing on the system are further discussed.

II. CLUSTER FORMATION AND FRACTAL PROPERTIES

As mentioned in the Introduction, the simulated LLV process shows intrinsically non-mean-field behavior. For relatively large lattices the system globally realizes a unique nonoscillatory steady state independent of the initial conditions, while locally the system presents oscillations of finite amplitude (Fig. 2).

To understand this unexpected feature one needs to look closely at the reaction scheme. Because all three reaction steps are autocatalytic, spontaneous formation of clusters of homologous particles is favored (see Fig. 3). In Fig. 3 the black particles represent X_1, the gray represent X_2, and the white particles represent empty sites. The reaction rates are $k_1=0.9$, $k_2=0.3$, $k_s=0.1$. Having started from random initial conditions, at a certain time $t=30$ MCS, formation of clusters of X_2 (Gray) is observed surrounded by empty sites (white) and a relatively small proportion of X_1 sites (black) between them. As time passes, $t=40$ MCS, some X_2 clusters grow, while others vanish. Note that the X_2 clusters that

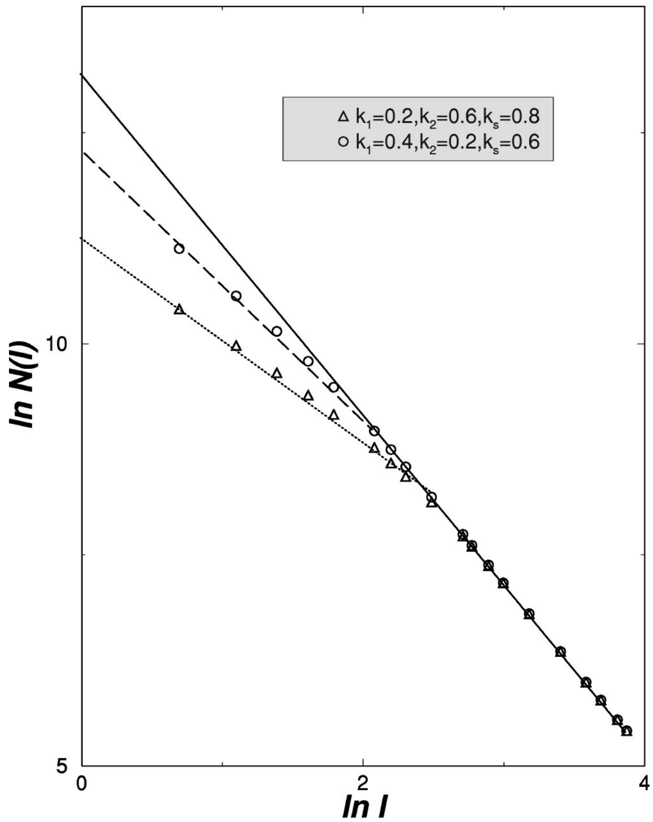

FIG. 4. Plot of the logarithm of number of boxes N containing at least one particle X_1 as a function of the logarithm of the box size ℓ for two different sets of the parameters. The solid line represents a power law with exponent $-d_f=-2$.

grow are in contact with X_1 clusters, which themselves propagate through the empty sites. Instead, X_2 clusters that are not "protected" by X_1 vanish. As time grows further, $t=50$ MCS, the X_2 clusters percolate the system while the empty regions are gradually reduced. At $t=60$ MCS, the entire lattice is invaded by X_2 while empty regions appear and start growing at the interior of the X_2 supercluster.

From this description of the development of fluctuations one can deduce that the origin of clusters are isolated sites or small clusters of one species, "left" within a large cluster of another species. Because reactions can take place only between different species, propagation of boundaries between clusters is the dynamical mechanism governing the process. This effect is more prominent when the reactivity rates are relatively different as in the case shown in Fig. 3.

To deduce whether or not the LLV system has spatial fractal properties the fractal dimension d_f is calculated using the box-counting method [34,35]. In order to ensure a large number of counts a 720×720 lattice was used. In Fig. 4 the value of $N(\ell)$ is plotted as a function of ℓ in a double-logarithmic scale, where $N(\ell)$ stands for the number of boxes of length ℓ covering the system and containing at least one X_1. The black triangles in this figure are for velocity constants $k_1=0.2, k_2=0.6, k_s=0.8$ while the circles are for $k_1=0.4, k_2=0.2, k_s=0.6$. The negative slope of those curves in double-logarithmic scale represents the fractal dimension of the system. It is quite clear that in the vicinity of $\ell_{up}\cong 40$–50 there appears to be a sharp change of slope. This is a characteristic length in our problem and does not show explicit dependence on the actual size of the lattice or on the initial conditions. Below the crossover length, ℓ_{up}, fractal local structuring is observed while above it the system resets to its original two-dimensional (2D) structure. The exact shape of the curves in Fig. 4 does not change with time after the system has reached the steady state. It is especially interesting to observe the change in slope shown in Fig. 4 that represent an abrupt change of dynamical behavior as one passes through the critical length scale, ℓ_{up}. The specific broken shape and the crossover to $d_f=2$ at sufficiently small scales of the curves in Fig. 4 indicate that the clusters have measurable interior and that only the boundaries can be approximately fractal.

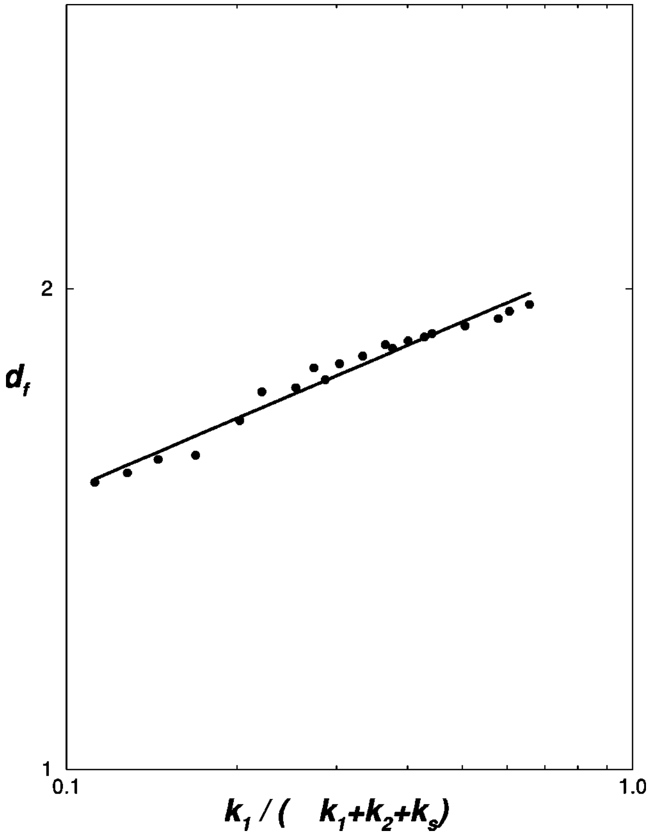

FIG. 5. The box-counting fractal dimension d_f as a function of $a_1=k_1/(k_1+k_2+k_s)$ in double-logarithmic scale. Each point represents the average on a number of counts. The standard error on each point for d_f is of the order of 0.04.

The fractal dimension for $1<\ell<\ell_{up}$ has been calculated using the box-counting method for different values of the parameters and the results are shown in Fig. 5. In double-logarithmic scale the curve is approximated by a power law of the form $d_f=Q[k_1/(k_1+k_2+k_s)]^p$. The exponent equals $p=0.151\pm0.006$. For consistency the value of Q must be equal to 2 since for $k_2=k_s=0$ the species X_1 covers the entire lattice and thus $d_f=2$. From the simulations the value of Q was found to be $Q=2.1$, which is within the acceptable error limits, due to the finite size of the lattice. Inversely, when $k_1\rightarrow 0$, X_2 species poisons the lattice and consequently the fractal dimension measured on the X_1 species is zero.

It appears that the parameter regulating d_f (as counted for the population X_1) is the quantity $a_1=k_1/(k_1+k_2+k_s)$, which is the effective parameter defined in Eq. (5). The results are taken after the system has reached its steady state and low values of d_f are computed when the system has low interaction probability for X_1. The same results were obtained when instead of X_1, X_2, or S is considered as the "active" population. This is expected because of the symmetries of the LLV model.

To calculate the degree of clustering in the system lacunarity analysis [34,36–38] is used that distinguishes between systems with different degree of "clumping." The lacunarity analysis used is based on the gliding-box algorithm proposed by Allain and Cloitre [36]. Square boxes of various sizes ($r\times r$) are placed on the system and the number $m(r)$ of sites within the box occupied by X_1 particles are recorded for different values of the box size r. The lacunarity is then defined as

$$\Lambda(r)=\frac{\langle m_s^2(r)\rangle+\langle m(r)\rangle^2}{\langle m(r)\rangle^2}, \tag{8}$$

where $\langle m_s^2\rangle$ is the variance of the number of X_1 particles per box.

Lacunarity was calculated for a 512×512 square lattice and for $k_1=k_2=k_3=0.8$ ($a_1=a_2=0.333$). The system was given enough time to reach its steady state (1500 MCS) and then lacunarity was computed for X_1 and the results are presented in Fig. 6 (solid line). For comparison, the lacunarity for a random set of the same lattice size and concentration was calculated (Fig. 6, dashed line). From Fig. 6, it is evident that the LLV has much higher lacunarity than the corresponding random set for all values of r thus indicating extensive clustering, a fact that is fully compatible with the "local oscillators" hypothesis. Analogous results are obtained for different values of the parameters (a_1,a_2) or equivalently (k_1,k_2,k_3).

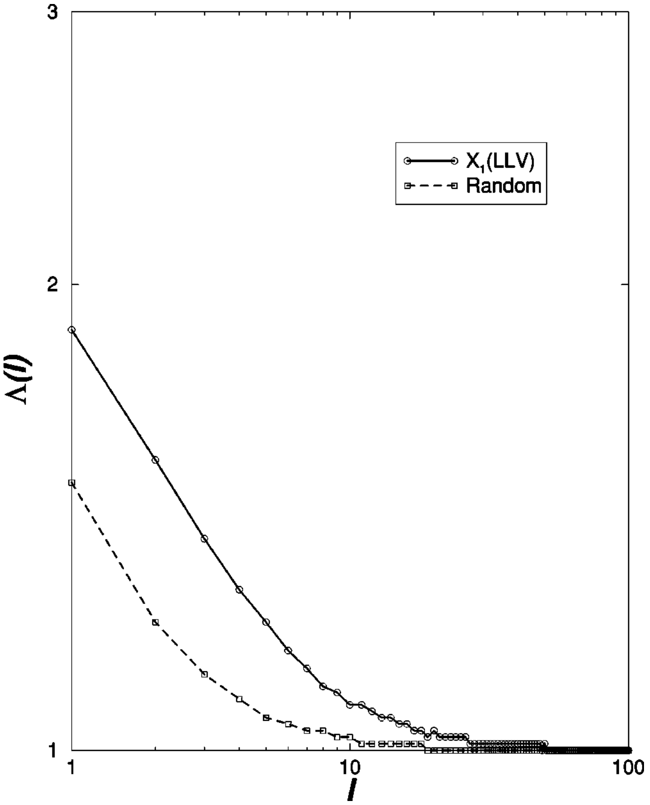

FIG. 6. Lacunarity Λ for species X_1 for the LLV model (solid line), and for a random set with the same concentration (dashed line) as a function of the block size ℓ. The graph is in double-logarithmic scale and the kinetic constants are $k_1=k_2=k_s=0.8$ ($a_1=a_2=0.333$).

III. FRACTAL SUBSTRATES

In a previous work [2] the LLV model was simulated via the Monte Carlo method on a linear 1D substrate and on a 2D square lattice. It was shown that on the 1D lattice the system never reaches the nontrivial mean-field fixed point, but after very long times only one of the three species survives depending on the kinetic constants and on the initial concentrations. Thus, in a 1D lattice, the oscillatory behavior is suppressed and the nontrivial steady state is never manifested. In contrast, for realizations on a 2D square lattice the nontrivial steady state is realized and oscillations are locally manifested. Dimensionality of the substrate seems to play a major role in the selection of the steady state. It is thus possible and technologically interesting to be able to control the outcome of the reaction by controlling the dimensionality of the substrate. Along these lines, there have been earlier experimental works on nanostructured catalysts [39] that demonstrate the effects of such fractal substrates on the catalytic properties of the surface. Also the effect of boundaries on catalysts of finite size has been studied [39].

Earlier simulations on fractal supports have been used to demonstrate the dramatic effects of the support geometry on various processes including chemical wave propagation on fractals [30], coupled map dynamics on fractal lattices [40], and chemical dynamics on fractal sets [3]. It is thus interesting to explore the behavior of the LLV dynamical system on self-similar substrates of fractional dimension D_s, $1\leqslant D_s\leqslant 2$. In such substrates each reacting particle has on the average fewer neighbors and thus less freedom for reaction than when the substrate is two dimensional. In the current work a fractal substrate is considered that consists of active and inactive sites. Both deterministic fractal (Sierpinski carpet) and random fractals are used with $D_s=1.893=\ln 8/\ln 3$. The three species X_1, X_2, and S are adsorbed only on the active sites, which constitute the fractal.

We implemented the LLV scheme onto three kinds of lattices (normal 2D square lattice, deterministic fractal, and random fractal). Due to the limitations in the number of nearest neighbors, during the evolution, one of the reactants would normally undergo a period of very low concentration. Then the fractal substrates can cause the total disappearance of this reactant and the catalytic surface will be poisoned by the remaining substance. This is demonstrated in Fig. 7 where the evolution of X_1 is presented for a normal 512×512 lat-

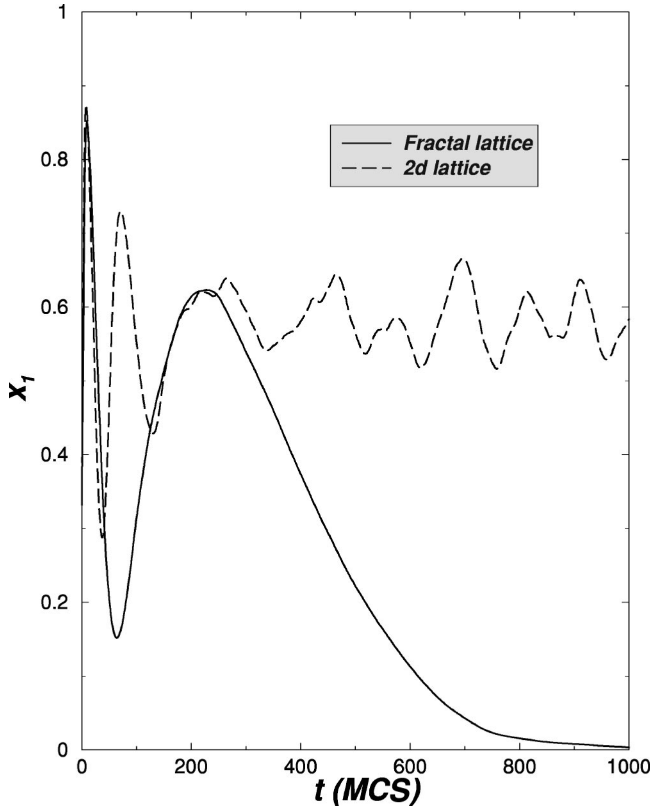

FIG. 7. Evolution of X_1 on a 2D lattice substrate (dotted line) and on a random fractal lattice (solid line). The 2D lattice size is 512×512 and the fractal lattice size is 729×729. The reaction constants are $k_1=0.9$, $k_2=0.3$, $k_s=0.1$ ($a_1=0.692$, $a_2=0.231$).

tice and a 729×729 fractal lattice ($D_s=1.893$) for $k_1=0.9, k_2=0.3, k_s=0.1$. These two particular lattice sizes were chosen in order to have the same number of active lattice sites. While in the 2D lattice X_1 is dominant, in the fractal lattice X_1 disappears. This poisoning phenomenon was not surprising since previous works [2] have shown that poisoning is always demonstrated by the 1D model. As the fractal substrates have dimension between one and two it can be expected that a reactive process on these substrates should also act as a hybrid between the 1D and the 2D model. No difference was observed between the random and the deterministic fractal substrate and it seems that the crucial factor regulating catalytic effects is the fractal dimension of the substrate as well as the statistical existence of boundaries and not its precise topology. It is also remarkable that in cases where the probabilities of the reactions were chosen close to each other, no significant effect of the fractal substrates was observed.

A logical explanation for the poisoning phenomena on fractal substrates may be as follows, reactions take place only within the border areas between clusters. The existence of impurities distributed in a fractal scheme upon the catalytic surface is triggering some boundary effects that involve the shrinking of the clusters because of the inactive areas introduced. When one of the species reaches a very low concentration, clusters of this species may be trapped in the borders of the fractal impurities and, as they will be unable to grow further, they will be ‘‘eaten up’’ by other species that will finally dominate. Note that for small values of k_2, X_1 particles are produced very infrequently; as a result X_2 attains very low concentrations and at a certain point, S can almost dominate the lattice by destroying all X_2. At the same time, the remaining clusters of X_1 start to grow and gradually they invade the entire lattice. By the same mechanism when low k_1 is considered, X_2 particles poison the lattice and when for low k_s, S dominate. When a fractal lattice is introduced the extra impurities—boundaries can enhance the above procedure thus extending the poisoning regions of the parameter space.

Figures 8 and 9 present the results from a set of LLV simulations that were performed with very low values of k_2 ($k_2=0.05,0.075$) and different values of k_1 and k_s for fractal ($D_s=1.893$) and 2D substrates. The lattice sizes are the same as in Fig. 3. In this domain of the parameters space poisoned states appear frequently. We investigated the effect of the dimensionality of the substrate in the poisoning phenomenon. The points marked with a box are the set of parameters for which X_1 poisoning is observed after $t=1500$ MCS while the circles represent X_2 poisoning at the same time. For the remaining (white) points oscillatory behavior was observed up to that time. In Fig. 8(a) $k_2=0.05$, which is relatively small and for most values of k_1 and k_s the system is poisoned with X_1. As the value of k_2 increases, Fig. 8(b), more-and-more oscillatory states appear at low values of k_1 and k_s. Similarly, in Fig. 9 the same tendency is observed for the poisoning of the 2D lattice. Comparison of Fig. 8 (fractal lattice) and Fig. 9 (2D lattice) shows that the poisoning states are more favored in the fractal lattice for identical parameter values. The change of the poisoning state due to the fractality of the substrate leads to the following conclusion: if one wishes to direct a system into a specific state without changing the kinetic constants it is enough to adjust the fractal dimension of the substrate appropriately.

IV. CONCLUSIONS

The lattice Lotka-Volterra model is studied using the mean-field approach and Monte Carlo simulations. In particular, the origin and development of local oscillators and clustering is studied using fractal and lacunarity analysis. In addition the effects of the fractal substrates on the dynamics of the system are studied. The main conclusions of this work are:

(1) There are indeed, as suggested in [2], spatial formations that act as local oscillators. We have concluded that those formations have fractal boundary structure and that the fractal dimension d_f depends on the reaction probabilities. Local oscillators have a characteristic length of about 40–50 lattice sites that is independent of the size of the lattice and shows very weak dependence on the reaction probabilities. High lacunarity is observed that indicates clustering of homologous species.

(2) The mean-field behavior is different from the Monte Carlo simulations due to local fluctuations that cause spatial formations.

(3) The oscillations are suppressed globally but are con-

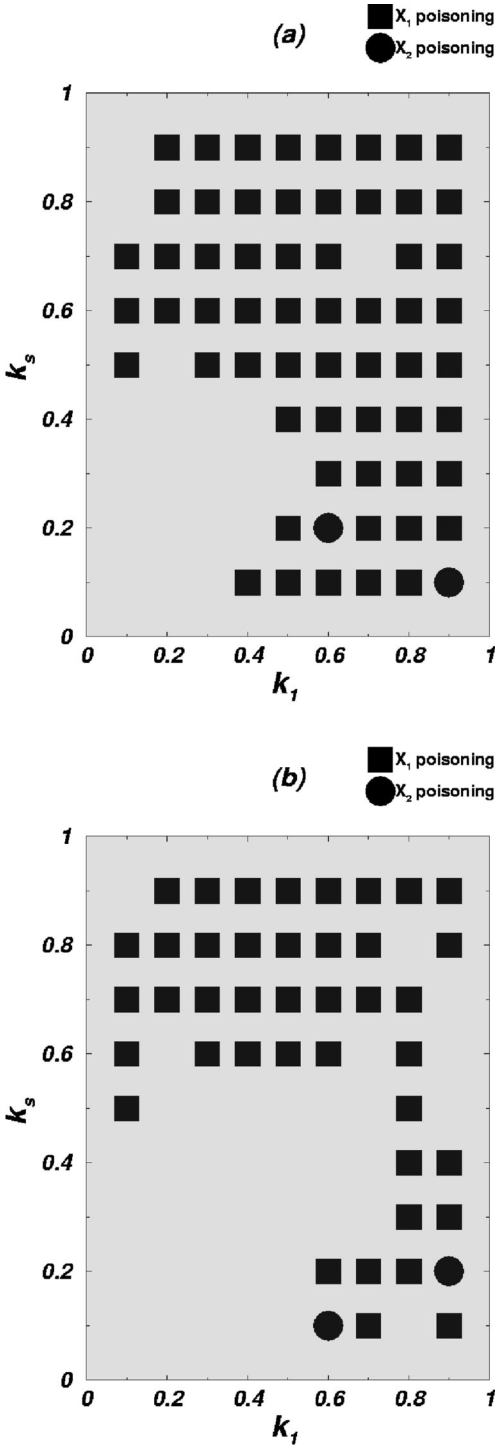

FIG. 8. Poisoning states for $k_2 = 0.05$ (a), $k_2 = 0.075$ (b), and k_1, k_s varying from 0.1 to 0.9. Black boxes represent X_1 poisoning, black spheres stand for X_2 poisoning, and the gray spaces correspond to oscillatory behavior. The simulations were performed on random fractal substrate with $D_s = 1.893$ for $t = 1500$ MCS.

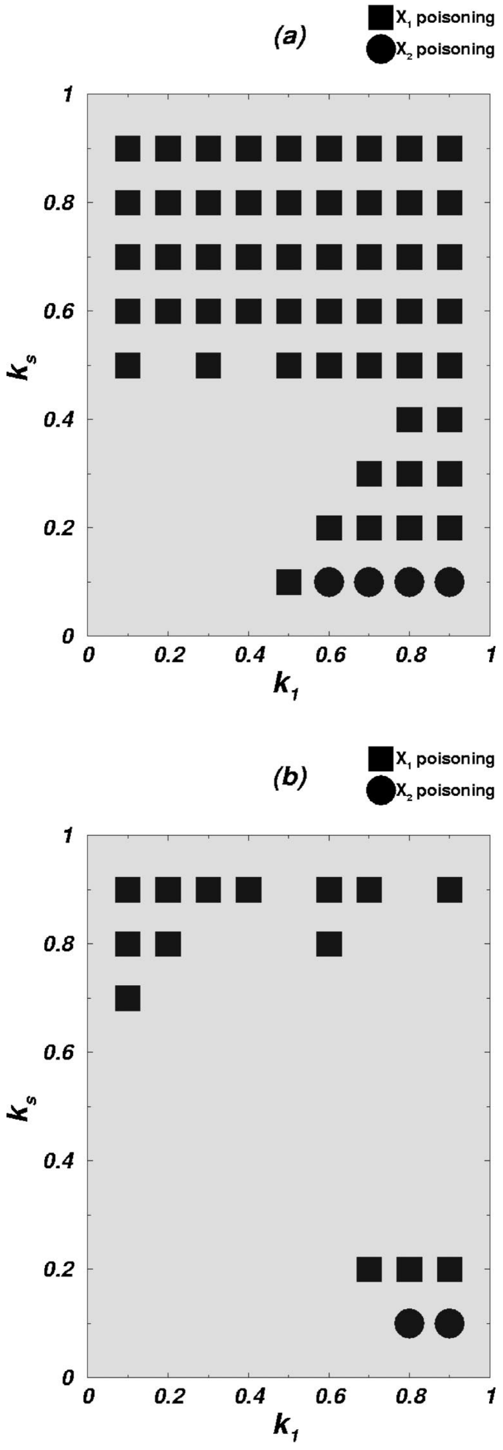

FIG. 9. Poisoning states for $k_2 = 0.05$ (a), $k_2 = 0.075$ (b), and k_1, k_s varying from 0.1 to 0.9. Black boxes represent X_1 poisoning, black spheres stand for X_2 poisoning, and the gray spaces correspond to oscillatory behavior. The simulations were performed on 2D substrate for $t = 1500$ MCS.

served locally. Because of the fact that the local oscillators have random phases, in large lattices no oscillations are observed around the steady state.

(4) For very large lattices the steady state demonstrated by the Monte Carlo method is very close (mean error of less than 6% depending on the lattice size and parameters) to the coordinates of the center as calculated from the mean-field theory. This indicates that when the problem is transferred on lattice globally this center is transformed to an attractor.

(5) Both random and deterministic fractal substrates dis-

play catalytic action on the LLV system especially when reaction probabilities differ significantly. This can even lead to poisoning of the catalytic surface by a certain reactant and could be used as a ‘‘selection filter.’’

The LLV model was tested under mixing conditions. This was performed by forcing each reacting particle to exchange positions with another random particle of the lattice. This procedure leads the system very quickly to its steady state and the oscillations are further reduced depending on the mixing rates.

The reverse model was also examined, namely,

$$2X_2 \xrightarrow{k_s} X_1 + X_2,$$

$$2S \xrightarrow{k_1} X_2 + S,$$

$$2X_1 \xrightarrow{k_2} X_1 + S.$$

The Monte Carlo simulations here produce exactly the same results as the mean field (the mean-field predicts an attractor). This is due to the fact that in the reverse model no local formations are supported and thus the whole lattice retains an excellent mixing (if a cluster is formed as a statistical fluctuation it is unstable and is soon destroyed).

Further studies on the LLV and on other minimal models are needed in order to clarify the mechanism under which the local oscillators are created and conserved and the influence of their local structure on the actual kinetics of the reactions. It is also an open problem to examine the use of fractal substrates as filters for specific reactants.

ACKNOWLEDGMENTS

The authors would like to thank Professors G. Nicolis, F. Baras, N. Antoniou, A. Malakis, and F. Diakonos for their valuable remarks and suggestions. We would also like to acknowledge stimulating discussions on the reverse model with Professor T. Bountis.

[1] G. Nicolis and I. Prigogine, *Self-organization in Nonequilibrium Systems* (Wiley, New York, 1977).
[2] A. Provata, G. Nicolis, and F. Baras, J. Chem. Phys. **110**, 8361 (1999).
[3] A. Tretyakov, A. Provata, and G. Nicolis, J. Phys. Chem. **99**, 2770 (1995).
[4] F. Baras, F. Vikas, and G. Nicolis, Phys. Rev. E **60**, 3797 (1999).
[5] R. Imbihl and G. Ertl, Chem. Rev. **95**, 697 (1995).
[6] V.P. Zhdanov, Phys. Rev. E **59**, 6292 (1999).
[7] H. Rose, H. Hempel, and L. Schimanksy-Geier, Physica A **206**, 421 (1994).
[8] G. Ertl, P.R. Norton, and J. Rustig, Phys. Rev. Lett. **49**, 177 (1982).
[9] M. Ehsasi, M. Matloch, O. Frank, J.H. Block, K. Christmann, F.S. Rys, and W. Hirschwald, J. Chem. Phys. **91**, 4949 (1989).
[10] R. Imbihl and G. Ertl, Chem. Rev. **95**, 697 (1995).
[11] M. Slinko, T. Fink, T. Loher, H.H. Madden, S.J. Lombardo, R. Imbihl, and G. Ertl, Surf. Sci. **264**, 157 (1992).
[12] C. Voss and N. Kruse, Appl. Surf. Sci. **87/88**, 127 (1994).
[13] C. Voss and N. Kruse, Ultramicroscopy **73**, 211 (1998).
[14] N. Hartmann, Y. Kevrekidis, and R. Imbihl, J. Chem. Phys. **112**, 6795 (2000).
[15] Th. Fink, J.-P. Path, M.R. Basset, R. Imbihl, and G. Ertl, Surf. Sci. **245**, 96 (1991).
[16] R.M. Ziff, E. Gulari, and Y. Barshad, Phys. Rev. Lett. **56**, 2553 (1986).
[17] B.J. Brosilow, E. Gulari, and Y. Barshad, J. Chem. Phys. **98**, 674 (1993).
[18] C.A. Voigt and R.M. Ziff, Phys. Rev. E **56**, R6241 (1997).
[19] E.V. Albano and J. Marro, J. Chem. Phys. **113**, 10279 (2000).
[20] P. Meakin, J. Chem. Phys. **93**, 2903 (1991).
[21] J.W. Evans and M.S. Miesch, Phys. Rev. Lett. **66**, 833 (1991).
[22] M. Tammaro and J.W. Evans, Phys. Rev. E **52**, 2310 (1995).
[23] V.P. Zhdanov, Surf. Sci. **426**, 345 (1999).
[24] D.-J. Liu and J.W. Evans, Phys. Rev. Lett. **84**, 955 (2000).
[25] V.P. Zhdanov, Phys. Rev. E **60**, 7554 (1995).
[26] H. Persson, P. Thormwälen, V.P. Zhdanov, and B. Kasemo, Catal. Today **53**, 273 (1999).
[27] J. D. Murray, *Mathematical Biology* (Springer-Verlag, Berlin, 1993).
[28] P. Grassberger, Math. Biosci. **63**, 157 (1983).
[29] J.M. Greenberg, B.D. Hassard, and S.P. Hastings, Bull. Am. Math. Soc. **84**, 1296 (1978).
[30] A.J. Irwin and S.J. Fraser, J. Chem. Phys. **93**, 3471 (1990).
[31] S. Fraser and R. Kapral, J. Chem. Phys. **85**, 5682 (1986).
[32] L. Frachebourg, P.L. Krapivsky, and E. Ben-Naim, Phys. Rev. E **54**, 6186 (1996).
[33] J. W. Turner (private communication).
[34] B. B. Mandelbrot, *The Fractal Geometry of Nature* (Freeman, New York, 1983).
[35] K. Falconer, *Fractal Geometry, Mathematical Foundations and Applications* (Wiley, New York, 1990).
[36] C. Allain and M. Cloitre, Phys. Rev. A **44**, 3552 (1991).
[37] R.E. Plotnick, R.H. Gardner, W.W. Hargrove, K. Prestegaard, and M. Perlmutter, Phys. Rev. E **53**, 5461 (1996).
[38] D.A. Fábio, A. Reis, and R. Riera, J. Phys. A **27**, 1827 (1994).
[39] F. Esch, S. Günther, E. Schütz, A. Schaak, I.G. Kevrekidis, M. Marsi, M. Kiskinova, and R. Imbihl, Surf. Sci. **443**, 245 (1999).
[40] M.G. Cosenza and R. Kapral, Phys. Rev. A **46**, 1850 (1992).